Journal of Mechanics Engineering and Automation 11 (2021) 135-148
doi: 10.17265/2159-5275/2021.05.003

Offshore Wind Power Evaluation Based on Nearshore Wind Power Correlations

Hsin-Chih Fang[1], Chien-Cheng Tu[2], Chao-Hong Lu[2] and Ta-Hui Lin[1,2]

1. Department of Mechanical Engineering, National Cheng Kung University, No. 1, University Road, Tainan City 701, Taiwan

2. Research Center for Energy Technology and Strategy, National Cheng Kung University, No. 1, University Road, Tainan City 701, Taiwan

Abstract: As the increasing number of wind energy is integrated into the national power grid, analyses of wind energy are becoming increasingly more crucial. The interaction between the topography and the northeast (*NE*) monsoon brings abundant wind resources to the Taiwan Strait in autumn and winter. The offshore area has stronger and more stable wind resources, so deployment of offshore wind power is also actively being carried out. However, development of offshore wind power systems requires stricter evaluation and decision-making. Therefore, this study implements a multi-site measurement verification to establish the relationship between the wind resources of the nearshore wind turbine system and a potential offshore power site in Chanbin. In the absence of a wind turbine at a specific location, potential of offshore wind energy is analyzed through wind resources. The findings showed that although the distance between these two sites is substantial, the nearshore and offshore areas at Chanbin experience similar wind conditions, and nearshore wind turbine can respond well to changes in wind speed and generate power accordingly. Afterwards, on this basis, the offshore power potential was evaluated and compared with the nearshore wind turbine systems. The results suggested the advantages of offshore wind power. A further analysis of the differences between power generation on a monthly basis was carried out to determine the distribution of wind turbine operation modes and illustrate the influence of the *NE* monsoon.

Key words: Chanbin, nearshore wind turbine system, offshore power potential assessment, *NE* monsoon, operation mode.

1. Introduction

Wind power systems extract kinetic energy from the wind using the wind turbine blade rotor. This energy is then transmitted to a generator through a transmission system to generate power. In 1919, the German physicist Betz used wind to flow through an idealized actuator disk, where it was found that the maximum energy that can be extracted from wind is 59.3%. This is the so-called the Betz limit [1, 2]. Nowadays, the blade efficiency of most wind turbines ranges between 20% and 40%.

Due to the shortage of fossil fuels, air pollution, and global environmental issues, many countries around the world have successively developed clean renewable energy. Although development of wind energy can mitigate these problems, there are also some challenges related to the integration of wind power, the most serious of which is wind energy intermittency. Wind energy has characteristics including high randomness, disorder and drastic changes. These issues, which are inherent in nature, induce the fluctuations in the national power grid, thereby influencing the reliability and safety of the grid and having impacts on energy management policies [3, 4].

In addition, setting up a power generation system requires a lot of time and is expensive. The locations of wind power plant and related facilities therefore must be carefully considered. Taiwan's high dependence on imported energy makes the country's economic development vulnerable to international situations, so it is urgent to develop self-produced energy. Therefore, the government has launched an energy policy focused on wind energy called the Four-Year Wind Energy Promotion Plan in the hope

Corresponding author: Hsin-Chih Fang, master's degree, research field: development of wind energy.

of accelerating the development of wind energy [5].

According to a global 23-year average wind speed observation study released by 4C offshore in 2014, the Taiwan Strait has 16 of the world's top 20 best offshore wind farms [6]. From north to south, the Bureau of Energy, Ministry of Economic Affairs released basic information on 36 potential wind power sites and related marine meteorological data in 2015 [7]. Potential site No. 26 planned in the Chanbin offshore area is discussed in this paper.

Compared with offshore areas, the development of nearshore wind power systems is becoming increasingly saturated. This paper discussed the No. 27 wind turbine inside the Chanbin Wind Power Station located in Changhua Coastal Industrial Park and analyzed its related wind resource data and its power generation status. This is compared with the wind resources of the No. 26 site to determine the potential for offshore wind power in Chanbin. This study is then extended to a discussion of the wind turbine models that are expected to be used at the potential offshore site.

Furthermore, the influences of the *NE* monsoon are analyzed based on the distribution of different operation modes of wind turbine in each month.

2. Methodology

2.1 Measurement Setup

As shown in Fig. 1, this study involved the nearshore and offshore sites in Chanbin. In terms of the offshore sites, a meteorological mast (24°00′3.44″ N, 120°16′22.62″ E) operated by Taipower Company was set up near the No. 26 potential offshore site. At the nearshore site, the No. 27 wind turbine was studied (24°09′28″ N, 120°25′46″ E). This data was combined with the measurement data obtained using Light Detection and Ranging (LiDAR) in front of the wind turbine.

2.1.1 Meteorological Mast

The meteorological mast was completed by Taipower Company in April 2016. The total height of the structure is 110 m, with 95 m above sea level and 15 m underwater.

Five anemometers and four wind vanes were installed at heights of 10, 30, 50 and 95 m above sea level.

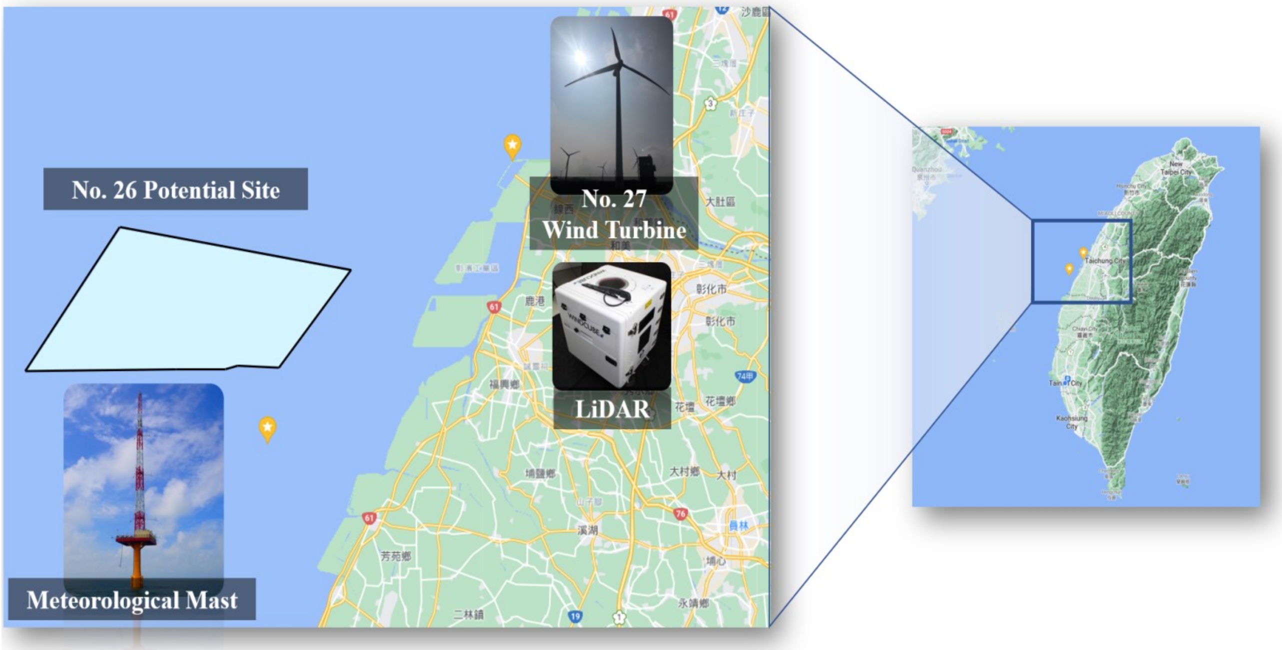

Fig. 1 Locations of the No. 26 potential offshore site, the meteorological mast, the No. 27 wind turbine, LiDAR in the Chanbin area.

According to the Wind Power Offshore System Demonstration Incentive Regulations formulated by the Ministry of Economic Affairs, in addition to wind speed and wind direction, measurement items must also include temperature, pressure, humidity, rainfall, net radiation intensity, wave height, wave period, wave direction, and other data. The corresponding measurement devices have also been installed. This mast is intended to collect marine meteorological data near the potential offshore site and establish a long-term wind resource database.

2.1.2 No. 27 Wind Turbine

Taipower Company divided the construction of a total of 31 wind turbine units at Chanbin Wind Power Station into two phases and plans to put them into commercial operation. This study involves the No. 27 wind turbine, which is located at the division between the land and the sea. This turbine is a Vestas V80-2.0MW model with a hub height of 67 m. The detailed specifications are provided in Table 1.

The wind resource data were measured by an anemometer on the nacelle of the wind turbine. The power data were obtained by the No. 27 wind turbine.

2.1.3 LiDAR

In addition, the offshore wind team of the Research Center for Energy Technology and Strategy (RCETS) set up LiDAR to measure the wind speed in front of the No. 27 wind turbine, as shown as Fig. 1. LiDAR is another wind measurement tool that can obtain vertical wind profile through a non-contact method by calculating the wind speed and direction at a specific height through the Doppler shift [8]. Unfortunately, the time span of the use of LiDAR was only from November 12, 2019 to December 31, 2019. Therefore, the measurement data from LiDAR could only be used to analyze the reliability of the anemometer.

The collection of the remaining dataset, including the offshore wind resource data, nearshore wind resource, and power data took place in 2019. The temporal resolution was 10-min. The summary of the data collection is presented in Table 2.

Table 1 Detailed specification of the No. 27 wind turbine.

Specification	Parameter value
Model	Vestas V80-2 MW
Rated power (P_R)	2 MW
Swept area	5,027 m^3
Power control	Pitch control
Cut-in speed (V_I)	4.5 m/s
Rated speed (V_R)	15.5 m/s
Cut-off speed (V_O)	25 m/s

Table 2 Data coverage.

Device	Location	Time span
Anemometer	Nearshore	2019
Turbine	Nearshore	2019
LiDAR	Nearshore	From Nov. 12, 2019 to Dec. 31, 2019
Mast	Offshore	2019

2.2 Data Pre-processing

2.2.1 Offshore Wind Speed Interpolation

As mentioned previously, five anemometers were installed on the Taipower meteorological mast at heights of 10, 30, 50 and 95 m, respectively. However, for the anemometer on nacelle of the No. 27 wind turbine and LiDAR, the height of the measurement data is 67 m corresponding to the hub height of the No. 27 wind turbine. Unfortunately, there are no data at the height of 67 m on the mast.

However, in general, the wind speed will increase with height. Therefore, there are two methods that can be used to depict the relationship between wind speed and height: the power law wind profile and logarithmic law wind profile [9, 10]. In this paper, the power law was used to interpolate the wind speed to the desired height, namely, the hub height of the wind turbine of interest in this paper. As shown in Eq. (1), α is wind shear exponent depending on surface roughness and atmospheric stability; V and h are wind speed and height used in the measurement data, and subscripts (1, 2) are two different heights above the surface.

Therefore, an offshore wind speed dataset with a height of 67 m is interpolated using the power law, so that the measurement height of the wind resource dataset remains consistent.

$$\frac{V_2}{V_1} = \left(\frac{h_2}{h_1}\right)^{\alpha} \tag{1}$$

2.2.2 Actual Power Data Treatment

Because of erroneous data collection system records, environmental noise factors, abnormality in wind turbine control systems, power generation control strategies, or other unspecified reasons, the collected dataset will be incomplete, and there will be outliers such as missing data, unnatural values, irrational values, etc. With so many problems, to reduce the uncertainty of the raw dataset, the dataset must be processed to modify and eliminate these invalid data.

In Ref. [11], Yun et al. summarized the preprocessing description and the distribution of outliers in their own datasets from Refs. [12-17]. Before we explore the raw data, it is necessary to be aware that it is impossible to ensure that all outliers are removed or processed completely. Wind turbines may develop different power generation behaviors in different locations and in different environments, even if the wind turbine model is the same. When different authors are dealing with their own datasets, the preprocessing will completely depend on the author's own definition of outliers. This manual method is the most direct and simplest method to perform data preprocessing. However, there may be some outliers hidden in the processed dataset [11]. What we can do is to distinguish the outliers as much as possible and increase confidence in the processed dataset. The statistical information is presented in Fig. 2.

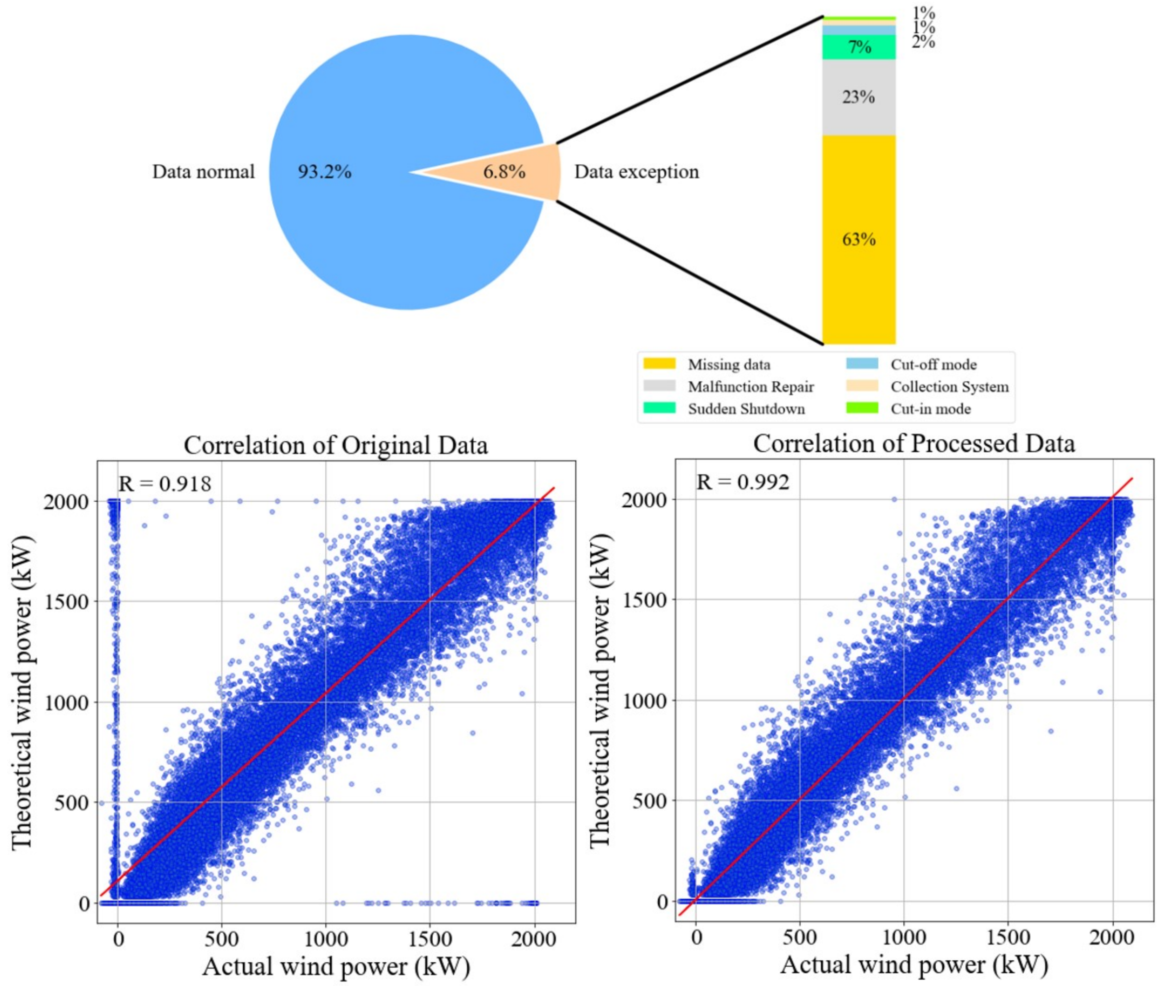

Fig. 2 Proportion of data classification at data preprocessing, power data correlation before and after preprocessing.

Among the data to be processed, the missing data account for the largest proportion. This may be due to faulty measurement instruments or the transmission issues. Another reason may be faults in the wind turbine operation. This problem occurred in November and December, which corresponds to the months with high wind speed. To protect wind turbines, when the wind speed exceeds V_O, the control system will stop the wind turbine. However, during the period that the wind speed fluctuates near V_O, the control system may fail, and wind turbine cannot be restarted. As a result, the wind turbine runs abnormally.

Other reasons include collection of wrong data, improper operation of the wind turbine, and issues with the power generation control strategies. When a wind turbine restarts for various reasons, the power generation will initially be relatively small. In addition, in not all situations, wind turbine can operate normally online. In some cases, the strong wind is blowing in the wrong direction, that is, it does not face the normal direction of the wind turbine rotor plane, so the wind turbine cannot response well to the wind speed.

Among these invalid data, if there are no more than two consecutive empty data units, that is, the time period in which there is invalid data is within 20 min; this situation can be replaced by the moving average and interpolation to fill in the missing data. If the empty period exceeds this threshold, these kinds of data need to be directly eliminated. Otherwise, forcible filling in the data may cause data distortion and lead to uncertainty in the data analysis.

2.2.3 Power Curve

The power curve plays an important role in wind power prediction, wind turbine control, power potential evaluation, and so on. Generally, it can be provided by the turbine manufacturer. The power curve and corresponding operation modes are shown in Fig. 3 and Table 3.

The power curve is divided into four operation modes using three critical wind speeds: V_I, V_R, and V_O. In the cut-in mode, the wind speed is the lowest. The low wind speed is not adequate to maintain the ability of the wind turbine to generate power. Whenever the wind speed is slightly higher and close to V_I, the control system will judge whether the wind speed is adequate to enable the wind turbine to generate power stably.

In the normal mode, the wind turbine can generate power when the wind speed is stable and above V_I. However, the wind power is proportional to the cube of wind speed in this mode, shown in Eq. (2). Once the wind speed changes significantly, the wind power will fluctuate more actively. This is one of the reasons why wind energy is intermittent.

$$P = \frac{1}{2} C_p \rho A V^3 \tag{2}$$

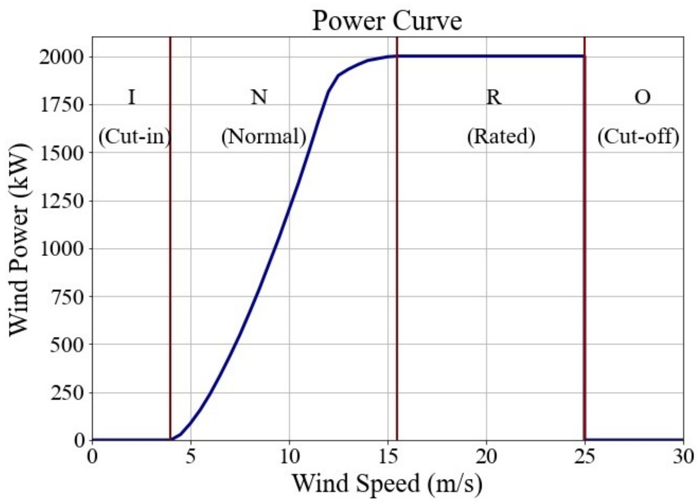

Fig. 3 The power curve of the No. 27 wind turbine (Vestas V80-2MW).

Table 3 The operation mode of the No. 27 wind turbine.

Wind speed (m/s)	Operation mode	Power generation
0 < WS < 4.5	Cut-in (I)	0
4.5 ≤ WS < 15.5	Normal (N)	By interpolating the power curve
15.5 ≤ WS < 25	Rated (R)	2 MW
25 ≤ WS	Cut-off (O)	0

In the rated mode, to protect the wind turbine, power generation will be restricted to the maximum power, that is, the rated power P_R. To respond to changes in wind speed in this region, two control methods have been developed: stall control and pitch control. The wind turbine studied in this study applies pitch control. When the wind speed becomes higher over time in this region, the pitch angle will adjust accordingly. As a result, part of the wind energy will be lost in order to maintain a fixed blade rotor rotation speed and generate P_R.

In the cut-off mode, once the wind speed is too fast, the resulting load exceeds the limit of the wind turbine. Therefore, the control system will actively brake the blade rotation and stop power generation until the wind speed is stably lower than V_O. This is the most difficult mode to analyze because of the complex control strategy.

In addition to assisting the data preprocessing to deducing the outliers, through the power curve of the No. 27 wind turbine, the nearshore wind speed can be converted to a theoretical power generation to compare it with the actual power generation. The theoretical power will respond to the change in wind speed to the greatest extent. It can reflect the responsiveness of the wind turbine. Also, the offshore power potential can be easy to obtain this way.

2.3 Research Process

At our research sites, there are many measurement devices to collect many datasets. Therefore, we implement the multi-site measurement verification to extend the research from nearshore to offshore and analyze the data from the wind speed to the wind power. Then, we evaluate the power potential at the offshore site. Fig. 4 shows the research process.

2.3.1 Measurement Reliability of the Anemometer

Because the anemometer on the nacelle of wind turbine is behind the rotor plane, the measurement of wind speed is located at the downstream side. Apart from other additional factors, the anemometer will be directly affected by the rotating rotor, which may cause errors in the measurement. Therefore, the propose of setting up LiDAR is to compare the results with the anemometer.

As mentioned before, the time span of LiDAR was only from November 12, 2019 to December 31, 2019. The dataset was too small to support the analysis with wind power. This LiDAR dataset was only to show the feasibility of the wind speed data measured by the anemometer.

2.3.2 Responsiveness of the Wind Turbine

The power curve provides the maximum power that a wind turbine can generate at different wind speeds. However, wind turbine blade rotor has greater mass and inertia, and wind turbines have different operation modes in different ranges of wind speed, which may also be affected by unusual human interference and

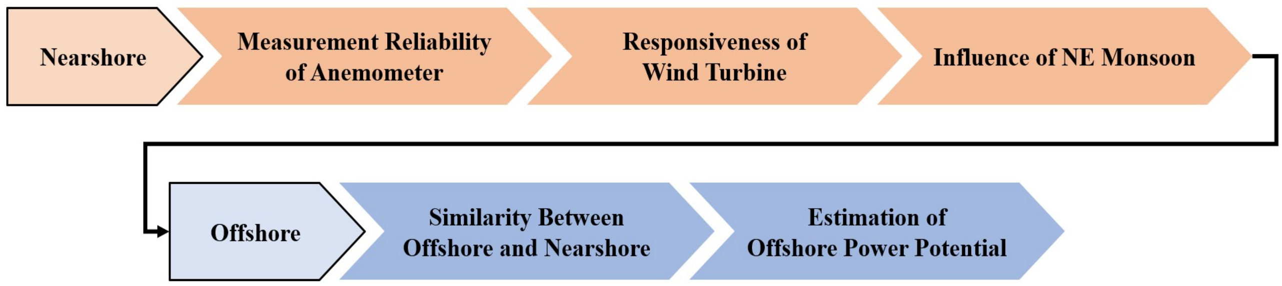

Fig. 4 Flow chart of research.

environmental noise. With so many problems, it is difficult for wind turbines to respond perfectly to changes in wind speed in order to generate power.

In this section, the actual power generation is compared with the theoretical power converted using the power curve to analyze the ability of wind turbine to response to changes in wind speed.

2.3.3 Influence of the *NE* monsoon

The Taiwan Strait is sandwiched by mountains and lies in the northeast-southwest direction. A strong northeast monsoon prevails in autumn and winter that affects the wind turbine power generation mode in different months.

According to the statistical results of the different wind turbine operation modes for every month, it is possible to determine the influence of the *NE* monsoon on wind power generation.

2.3.4 Offshore and Nearshore Similarities

Evaluation of offshore power potential is one of the vital purposes of this paper. Nearshore wind power system has become saturated. Based on this, the actual nearshore wind power situation can provide a crucial basis for offshore evaluation. However, it is necessary to first ensure that there are similar wind conditions at offshore and nearshore sites based on the premise that these two sites are 23.6 km apart.

Fortunately, unlike onshore site, the nearshore area is located at junction of the land and the sea. In addition, the site located at the sharp corners where the land extends into the sea, so the impact from the land is relatively low.

2.3.5 Evaluation of Offshore Power Potential

Based on the similarity between the offshore and nearshore sites and responsiveness of wind turbine, the relationship between the offshore and nearshore sites and the relationship between wind speed and power generation can be established. Then, offshore power potential can be easily assessed. A lot of power curve modeling has been proposed to make wind energy evaluations more accurate [11]. However, in this paper, the power curve is used to convert the wind speed to the theoretical power. It is the simplest and most intuitive simulation method.

In spite of the fact that there are too many factors influencing actual power generation, this method can give a clear understanding of offshore power potential and likely power situations.

3. Results and Discussions

3.1 Wind Speed Correlation between the Anemometer and LiDAR

In this section, it is necessary to ensure the reliability of the anemometer on the nacelle of the wind turbine and to ensure that the wind speed measured by the anemometer ($WS_{Ane.}$) will not be seriously affected by the rotating rotor.

$WS_{Ane.}$ is compared with the wind speed measured using LiDAR (WS_{LiDAR}) for the period from November 12, 2019 to the end of the year. As shown in Fig. 5, the wind speed measured by the two measurement tools exhibits a similar trend. Despite the fact that the anemometer is located behind the downwind side of the wind flow, and the rotating rotor may have a greater impact, the actual measurement results indicate that the influence is not significant.

According to the difference analyses for the wind speed data, there is a difference between the positive and negative cases that show that WS_{LiDAR} is higher and lower than $WS_{Ane.}$, respectively. $WS_{Ane.}$ is slightly smaller than WS_{LiDAR}. There is no doubt that the downstream wind speed will still be slightly affected by the rotor, and the wind speed may inevitably decrease. However, this influence is not obvious. Consequently, $WS_{Ane.}$ is reliable was considered adequate to support the subsequent comparison with wind power.

Also, whenever the wind speed is relatively small, the difference is also accordingly small and increases with increases in the wind speed. On the one hand,

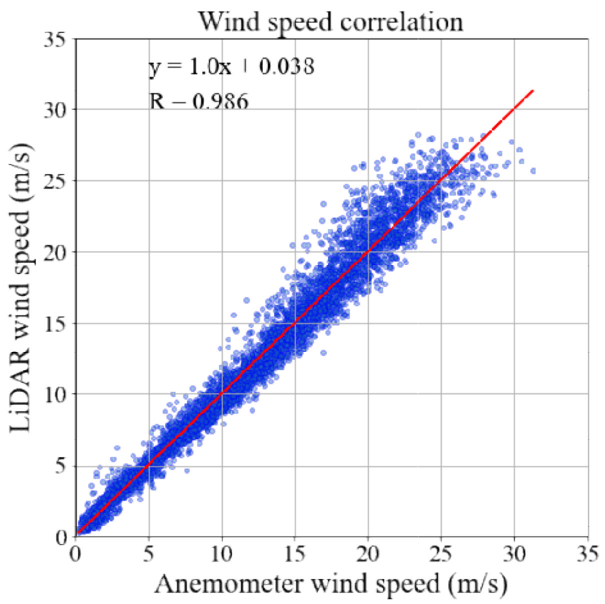

Fig. 5 Wind speed correlation between the anemometer and LiDAR.

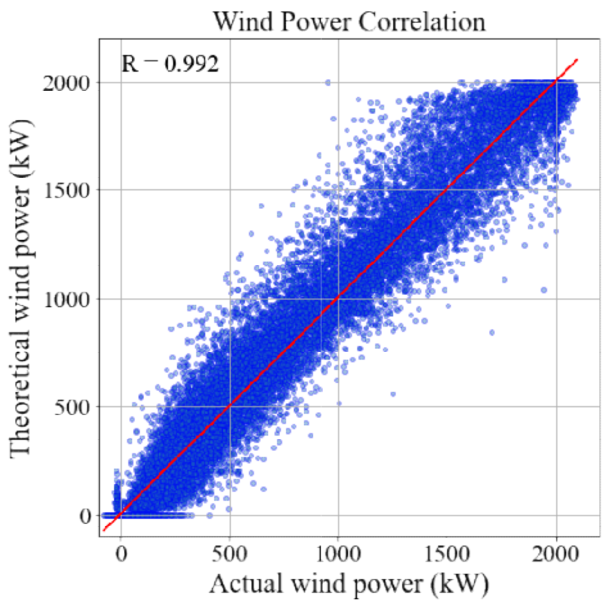

Fig. 6 Wind power correlation between the actual and theoretical power.

when the wind speed is low, the rotation speed of the blade rotor is also slow or stops. Conversely, when wind speed is high, the rotor speed is fast. Thereby, the measurement of the wind speed is also seriously affected.

These differences in the trends in the wind speed data provided good information for the subsequent wind power analysis. When the wind speed is high and exceeds V_R, the wind turbine control system generally has to the protect wind turbine, and only P_R will be generated. Even if the difference between the wind speed data is significant, there will not be much difference in the power generation.

3.2 Actual and Theoretical Power Correlations

The simplest power simulation is to convert the wind speed to the theoretical power through the power curve. This method can reflect possible power potential directly and show distribution of the operation modes. In Section 2.2.2, the invalid data were removed from the raw power dataset to reduce the data uncertainty.

At first glance, wind turbine can response the changes in wind speed well to generate power, as shown in Fig. 6. Therefore, actual power generation can fit the theoretical values mostly. Although this result is expected, it also provides us with a more reliable evidence for the subsequent analysis. Offshore power potential can be evaluated by power curve reasonably.

In actual situations, negative power generation is normal, where regardless of whether the wind speed is too low or too high, the wind turbines cannot generate power, as mentioned in Section 2.2.3. Data collection will record the net power generation; that is, the recorded data will include the power consumption of other auxiliary components of the wind turbine system. When the wind turbine is not in the power generation mode, the normal and rated modes, the power generation is not adequate to offset the consumption by other auxiliary components of the wind turbine.

Furthermore, during the periods of low wind speed, the wind speed is gradually decreasing; that is, operation mode of wind turbine goes from the normal mode to the rated mode. Although the wind speed is not adequate to support power generation, due to the large mass and inertia of the blades, the blades still can rotate continuously. As a result, the wind turbine can generate a small amount of power.

On the whole, the actual power generation was similar to the theoretical value. However, there still were some clear exceptions. This may have been due to significant wind speed changes that caused the wind turbine to fail to respond quickly and the power to fluctuate rapidly. Since the stability of the power supply cannot be ensured, this is the main reason why wind energy cannot become the base load power, especially for large-scale wind energy integration. However, it is undeniable that there are rich wind resources in Taiwan, so wind energy can mitigate the energy supply dilemma in Taiwan.

3.3 Influence of the NE monsoon

Taiwan has the best wind farms in the world due to the interaction between the *NE* monsoon and the topography. Although the *NE* monsoon blows throughout the year, its intensity weakens in spring and summer, and a great mass of southwest winds exists in these periods.

Fig. 7 shows the nearshore average wind speed and power generation for each month in 2019. There are the similar trends between the wind speed and wind power. When the wind speed is high, more power is generated simultaneously. Meanwhile, the higher values of both occur at the beginning and end of year, which corresponds to the greater influence of the *NE* monsoon.

Table 4 shows the occurrence ratio of wind turbine operation modes. From September to December and from January to February are the periods that the *NE* monsoon has the most effects (the *NE* season). The power generation composition is mostly in the normal and rated mode. In contrast, from April to August, the month that the *NE* monsoon has the least effects (the non-*NE* season), the power generation is mostly composed by the cut-in and normal mode. This clearly shows that more power can be generated during the *NE* season.

In addition, the cut-off mode only occurs in the *NE* season. Despite the fact that it reduces the average power, it also proves that the most abundant wind resources are available mainly in the *NE* season.

3.4 Offshore and Nearshore Wind Speed Correlations

Because the nearshore wind turbine is installed at the junction of the land and the sea, it is relatively less affected by land disturbance and may share similar characteristics to offshore conditions. Therefore, if the results of this analysis are valid, the potential for offshore power generation will be reasonably assessed.

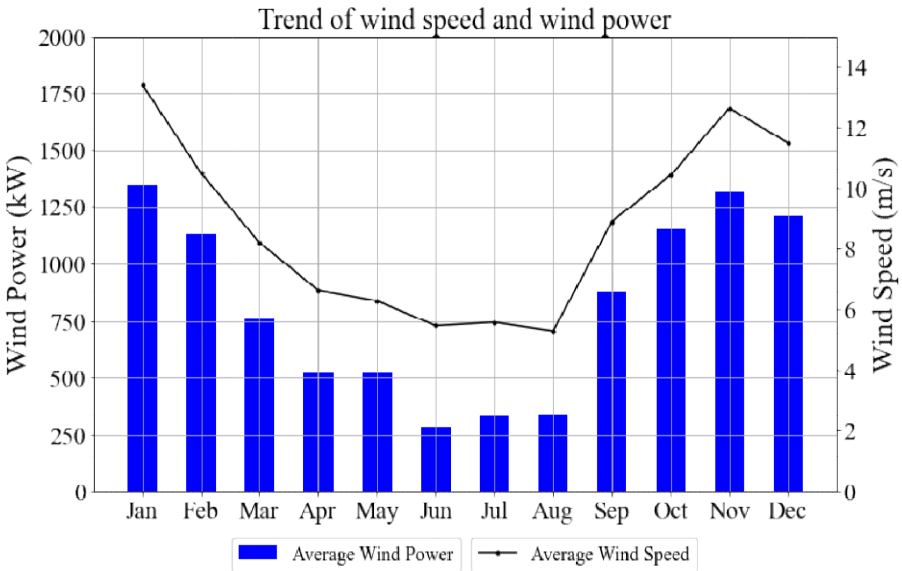

Fig. 7 Average wind speed and wind power distribution in the Chanbin nearshore area.

Table 4 Occurrence ratio of wind turbine operating modes.

Month	Operating modes (%)			
	I	*N*	*R*	*O*
Jan.	5.10	42.17	**50.10**	2.62
Feb.	13.71	56.60	**29.69**	0.00
Mar.	**25.61**	56.01	18.39	0.00
Apr.	**20.41**	70.75	8.84	0.00
May	**31.31**	58.16	10.53	0.00
Jun.	**18.81**	79.70	1.49	0.00
Jul.	**20.68**	78.45	0.88	0.00
Aug.	**35.76**	59.22	5.01	0.00
Sep.	21.83	48.70	**28.31**	1.16
Oct.	13.24	46.53	**40.23**	0.00
Nov.	9.52	40.35	**50.00**	0.13
Dec.	10.32	48.90	**40.75**	0.03
Annual	19.29	57.38	22.99	0.34

Wind speed is the key to power generation, so possible offshore power generation situation can be assessed by comparing the wind resource data between offshore and nearshore sites. The dataset shown in Fig. 8 covers 2019. Although these two sites are 23.6 km apart, as shown in Fig. 1, there is still a very high correlation. Apparently, these two sites experience similar wind condition.

Also, according to the difference in the wind speed data between the nearshore and offshore sites, the positive difference is greater than the negative difference. Although the overall trends are similar, there is no denying that the offshore wind speed is still higher than the nearshore wind speed due to less interference from land.

Fig. 9 shows the wind speed distribution for the offshore and nearshore sites. Compared to the nearshore condition, the distribution in the low wind speed region in the offshore area is less; that is, it transfers to the medium or high wind speed regions. This suggests that the proportion of higher wind speeds offshore is greater than that in the nearshore area.

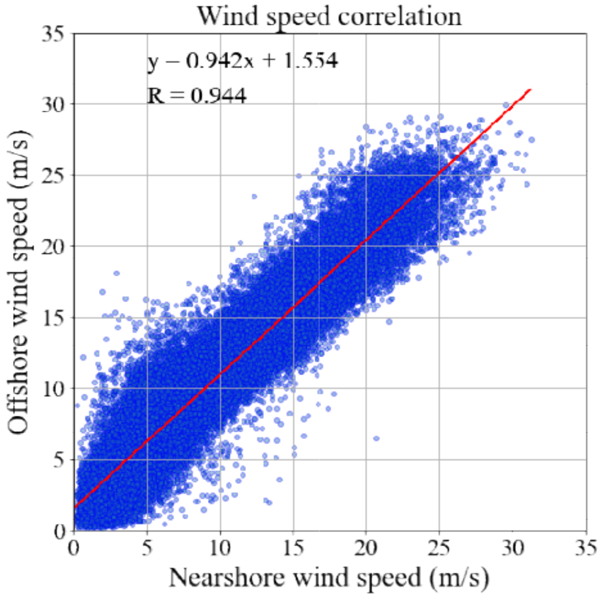

Fig. 8 Wind speed correlation between the offshore and nearshore Chanbin areas.

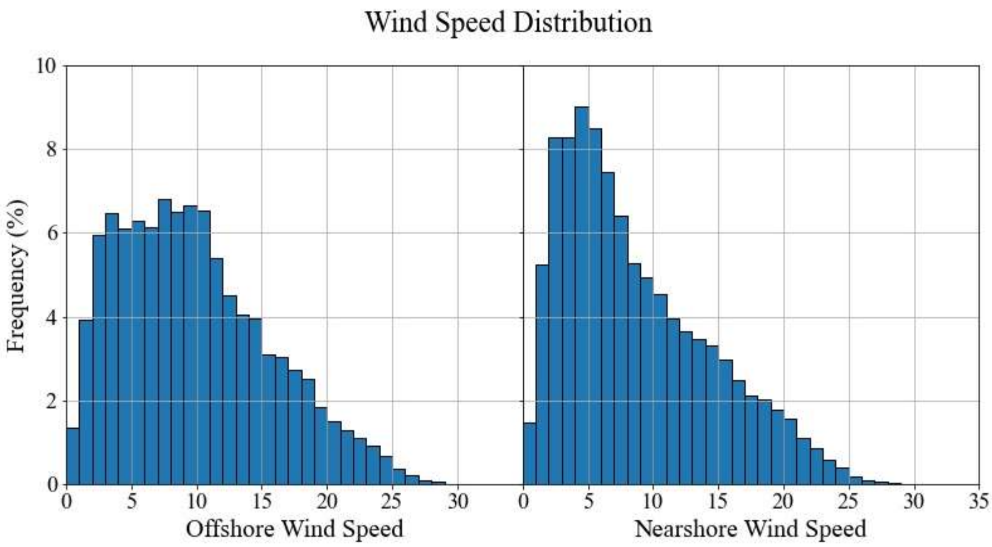

Fig. 9 Wind speed distribution at the Chanbin nearshore and offshore site.

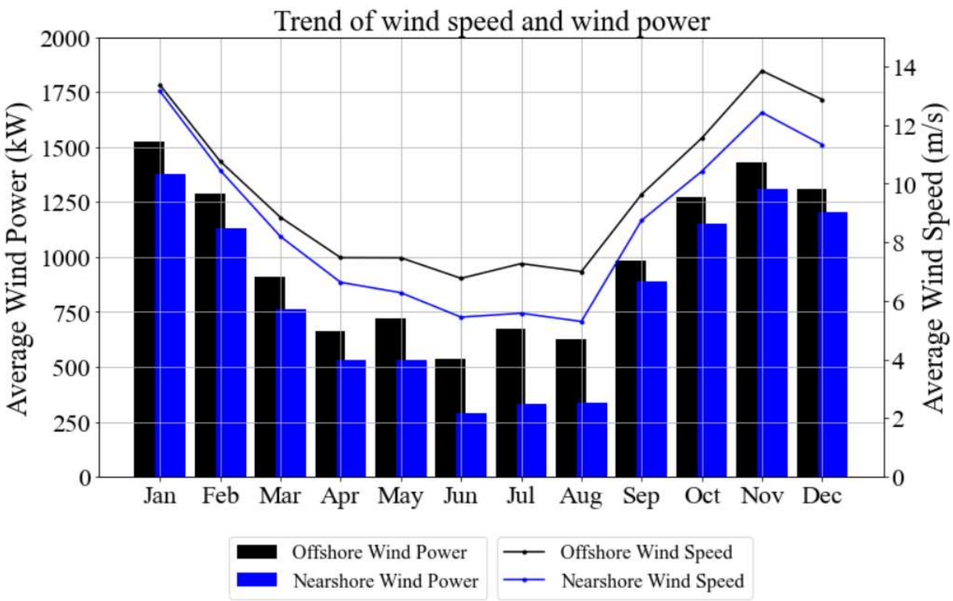

Fig. 10 Average wind speed and wind power distribution at the Chanbin nearshore and offshore area.

3.5 Evaluation of the Offshore Power Potential

As mentioned above, the wind speeds for the offshore and nearshore sites are highly correlated, which means that they experience similar wind conditions. Furthermore, wind turbine can respond well to changes in wind speed and generate power according to the power curve. Therefore, the offshore power potential can be easily assessed by converting the offshore wind speed through the power curve to determine possible offshore power.

The results of the offshore average wind speed and power potential shown in Fig. 10 were compared with nearshore situations. Similarly, the higher average wind speed and possible power generation also occurred at the beginning and end of the year, which corresponds to the *NE* season. In other seasons, because of the lower wind speed, wind power is also relatively low.

Because offshore areas are less affected by land disturbance than nearshore areas, the average offshore wind speed is higher than the nearshore wind speed, and wind speed is the key to the wind power, especially in the non-*NE* season. The average wind speed increases nearly 2 m/s, but the power generation nearly doubles, as shown in Fig. 11.

Conversely, despite the fact that the average wind speed also increases 1 to 2 m/s in the *NE* season, a wind speed that is higher than V_R can only allow a wind turbine to generate P_R; therefore, the average wind power does not increase by much.

Also, although it is in the *NE* season, the wind speed differences between the nearshore and offshore sites in November and December are greater than those in January and February. However, the growth rate of the offshore power potential is similar. Logically, a higher wind speed leads to the ability of the wind turbine to generate more power, but it is essential to note the influence of the cut-off mode.

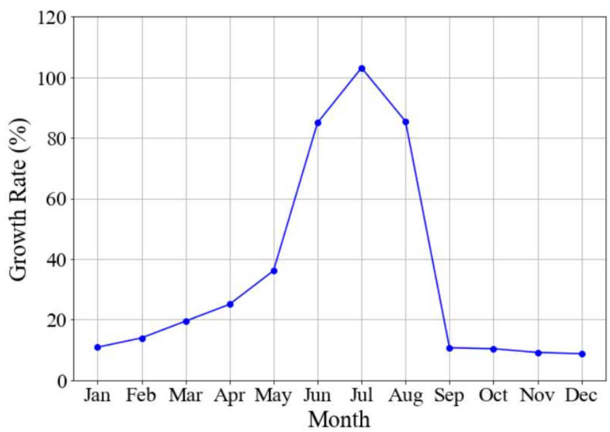

Fig. 11 Growth rate of offshore power compared with nearshore.

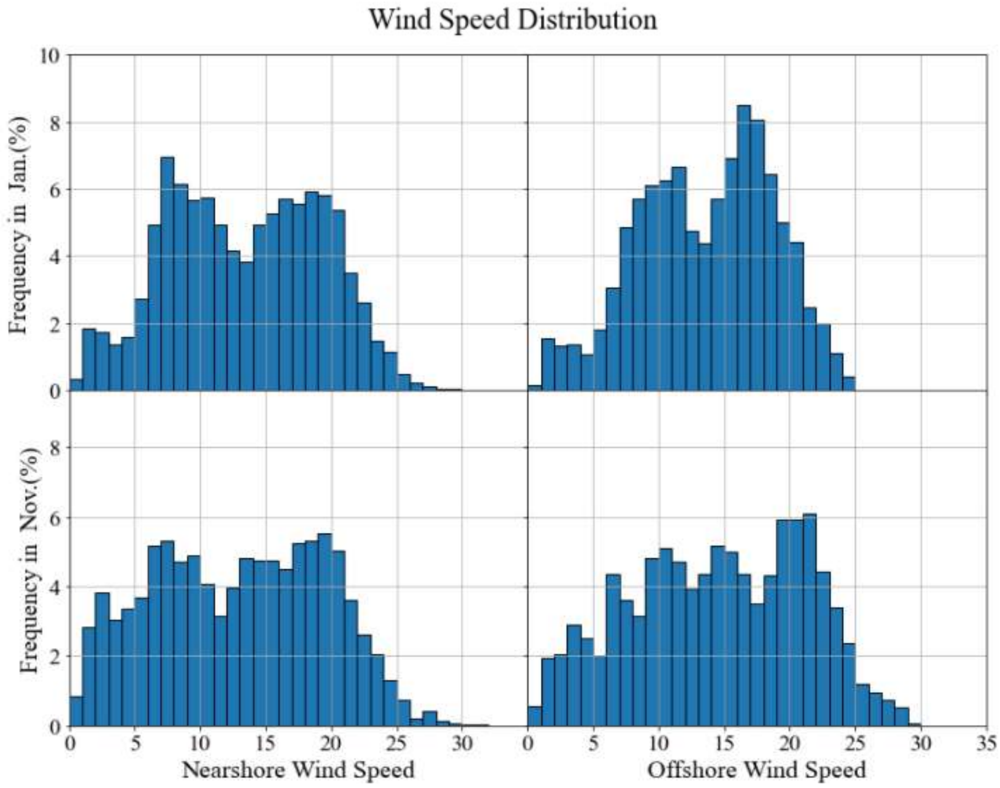

Fig. 12 Wind speed distribution in January and November.

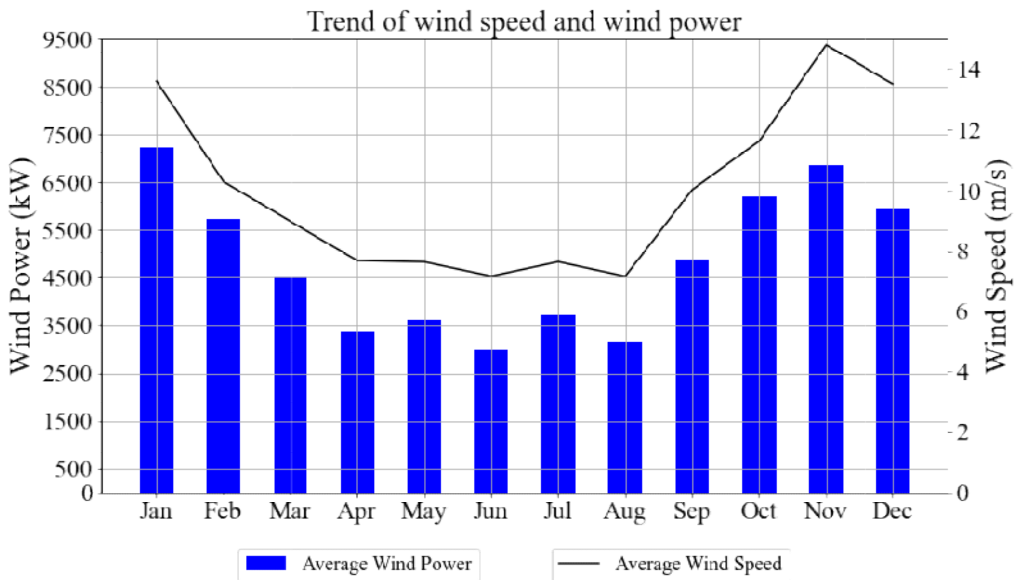

Fig. 13 Average wind speed and power potential distributions at Chanbin offshore potential site by using MHI Vestas V164-9.5MW.

Taking January and November as an example, the wind speed distribution is shown in Fig. 12. In January, the proportion of high wind speed in the offshore area is more than that at nearshore, and there is no wind speed exceeding V_O. That is, the cut-off mode will not impact the power generation or reduce the average power.

On the contrary, the wind speed difference between the offshore and nearshore is higher in November, because there are some wind speeds exceeding V_O. As a result, the average power generation is affected by the cut-off mode and in turns reduces the average power generated in November.

Finally, due to the richer wind resource at the offshore site, the 2 MW wind turbine model cannot satisfy the needs of the potential offshore site. Therefore, the investigation is extended by using the MHI Vestas V164-9.5MW, which is the more advanced wind turbine model used in offshore wind farms. The hub height was set at 95 m. A power curve of 9.5 MW wind turbine was used to evaluate the offshore power potential. The results are shown in Fig. 13.

There is no doubt that the trends in the wind speed and power generation are similar to the previous case. Because the wind speed for the meteorological mast at a height of 95 m is used, the average wind speed is slightly higher than that at the height of 67 m. However, it is important to note that the power generation of the 9.5 MW model is far greater than that of 2 MW model. Although an offshore wind energy system is more expensive and is time-consuming to build, the benefits it brings are also obvious.

4. Conclusions

Through the data collection systems, including the meteorological mast, the No. 27 wind turbine, and LiDAR, we collected many datasets and establish a database for the analysis of multi-site measurement verification.

Despite the distance of 23.6 km, there are still similar trends in the nearshore and offshore wind conditions that showed that the land has little influence on wind measurement. Except for abnormal data such as data collection errors and invalid wind turbine control strategies, although there are still some outliers, in general, wind turbines can respond well to changes in wind speed.

Finally, the offshore power potential was evaluated using the power curve and compared with actual nearshore conditions to reveal the advantage of offshore wind energy. The model was extended to use the MHI Vestas V164-9.5MW power curve in order to describe the expected power generation of the wind turbine at the potential site.

However, an entire wind farm comprises of many wind turbines, so an analysis of a single wind turbine is not adequate to support the development and deployment of offshore wind farms. Therefore, in the future, we will use Windsim or other wind power software to explore the power potential for an entire wind farm at an offshore site.

Acknowledgment

This research was financially supported in part by the National Science Council, Republic of China, under contract MOST 110-2221-E-006-183-. Moreover, it was supported by Taipower and RCETS offshore wind power team.

References

[1] Villanueva, D., and Feijóo A. 2010. "Wind Power Distributions: A Review of Their Applications." *Renewable and Sustainable Energy Reviews* 14: 1490-5.

[2] Jiang, H., Li, Y., and Cheng, Z. 2015. "Performances of Ideal Wind Turbine." *Renewable Energy* 83: 658-62.

[3] Ren, G., Liu, J., Wan, J., Guo, Y., and Yu, D. 2017. "Overview of Wind Power Intermittency: Impacts, Measurements, and Mitigation Solutions." *Applied Energy* 204: 47-65.

[4] Ren, G., Wan, J., Liu, J., Yu, D., and Söder, L. 2018. "Analysis of Wind Power Intermittency Based on Historical Wind Power Data." *Energy* 150: 482-92.

[5] Bureau of Energy, Ministry of Economic Affairs, R.O.C. 2017. "Four-year Wind Power Promotion Plan." https://www.moeaboe.gov.tw/ECW/populace/content/ContentDesc.aspx?menu_id=5493.

[6] 4C Offshore. 2021. "Global Offshore Win Speeds Rankings." https://www.4coffshore.com/windfarms/windspeeds.aspx.

[7] Bureau of Energy, Ministry of Economic Affairs, R.O.C. 2015. "Key Points of Application for Offshore Wind Power Planning and Site Application." https://www.moeaboe.gov.tw/ECW/populace/Law/Content.aspx?menu_id=2870.

[8] Shu, Z. R., Li, Q. S., He, Y. C., and Chan, P. W. 2016.

"Observations of Offshore Wind Characteristics by Doppler-LiDAR for Wind Energy Applications." *Applied Energy* 169: 150-63.

[9] Boopathi, K., Kushwaha, R., Balaraman, K., Bastin, J., Kanagavel, P., and Reddy Prasad, D. M. 2021. "Assessment of Wind Power Potential in the Coastal Region of Tamil Nadu, India." *Ocean Engineering* 219: 108356.

[10] Okorie, M. E., Inambao, F., and Chiguvare, Z. 2017. "Evaluation of Wind Shear Coefficients, Surface Roughness and Energy Yields over Inland Locations in Namibia." *Procedia Manufacturing* 7: 630-8.

[11] Wang, Y., Hu, Q., Li, L., Foley, A. M., and Srinivasan, D. 2019. "Approaches to Wind Power Curve Modeling: A Review and Discussion." *Renewable and Sustainable Energy Reviews* 116: 109422.

[12] Liu, Z., Gao, W., Wan, Y., and Muljadi, E. 2012. "Wind Power Plant Prediction by Using Neural Networks." In *Proceedings of the 2012 IEEE Energy Conversion Congress and Exposition (ECCE)*, 3154-60.

[13] Zheng, L., Hu, W., and Min, Y. 2015. "Raw Wind Data Preprocessing: A Data-Mining Approach." *IEEE Transactions on Sustainable Energy* 6: 11-9.

[14] Shen, X., Fu, X., and Zhou, C. 2019. "A Combined Algorithm for Cleaning Abnormal Data of Wind Turbine Power Curve Based on Change Point Grouping Algorithm and Quartile Algorithm." *IEEE Transactions on Sustainable Energy* 10: 46-54.

[15] Zhao, Y., Ye, L., Wang, W., Sun, H., Ju, Y., and Tang, Y. 2018. "Data-Driven Correction Approach to Refine Power Curve of Wind Farm under Wind Curtailment." *IEEE Transactions on Sustainable Energy* 9: 95-105.

[16] Bao, Y., Pan, D., Wang, X., Liao, L., and Yang, Q. 2017. "Least-Square B-Spline Approximation Based Wind Turbine Power Curve Modeling." In *Proceedings of 2017 Chinese Automation Congress (CAC)*, 6711-6.

[17] Sainz, E., Llombart, A., and Guerrero, J. J. 2009. "Robust Filtering for the Characterization of Wind Turbines: Improving Its Operation and Maintenance." *Energy Conversion and Management* 50: 2136-47.